Primljen / Received: 19.11.2015.
Ispravljen / Corrected: 13.4.2016.
Prihvaćen / Accepted: 25.8.2016.
Dostupno online / Available online: 10.3.2017.

Low temperature properties of hot mix asphalts prepared with different polymer modified binders

Authors:

Assoc.Prof. Taner Alataş, PhD. CE
Fırat University, Turkey
Faculty of Engineering
talatas@firat.edu.tr

Mesude Yilmaz, PhD. CE
General Directorate of Highways, Turkey
myilmaz7@kgm.gov.tr

Preliminary note

Taner Alataş, Mesude Yilmaz

Low temperature properties of hot mix asphalts prepared with different polymer modified binders

The low temperature crack propagation resistance of pure and polymer modified mixtures is analysed in the paper by means of linear and nonlinear fracture mechanics. The influence of two bitumen-modification binders is considered: styrene-butadiene-styrene (SBS) and ethylene-vinyl-acetate (EVA). The experiments demonstrated that the fracture toughness values increase, and the maximum vertical strain values decrease, with a decrease in temperature. It was established by both techniques used in the paper that the lowest fracture toughness was obtained using the EVA binder.

Key words:
hot mix asphalt, low temperature performance, modification, fracture toughness

Prethodno priopćenje

Taner Alataş, Mesude Yilmaz

Niskotemperaturna svojstva vrućih asfaltnih mješavina s različitim polimerom modificiranim vezivima

U radu se analizira otpornost čistih i polimerima modificiranih mješavina na širenje pukotina pri niskim temperaturama primjenom linearne i nelinearne mehanike loma. Razmatran je utjecaj dva veziva za modificiranje bitumena: stiren-butadien-stiren (SBS) i etilen-vinil-acetat (EVA). Ispitivanja su pokazala da pri padu temperature rastu vrijednosti lomne žilavosti, a smanjuju se vrijednosti maksimalne vertikalne deformacije. Ustanovljeno je da je u oba postupka primijenjena u ovom radu najniža vrijednost lomne žilavosti dobivena primjenom veziva EVA.

Ključne riječi:
vruća asfaltna mješavina, ponašanje pri niskoj temperaturi, modifikacija, lomna žilavost

Vorherige Mitteilung

Taner Alataş, Mesude Yilmaz

Eigenschaften heißer Asphaltmischungen mit verschiedenen durch Polymere modifizierten Bindemitteln bei tiefen Temperaturen

In dieser Arbeit wird mittels linearer und nichtlinearer Bruchmechanik der Widerstand reiner und mit Polymeren modifizierter Mischungen in Bezug auf die Rissausbreitung bei tiefen Temperaturen analysiert. Es wurden die Einflüsse von zwei Bundemitteln zur Modifikation des Bitumens betrachtet: Styrol-Butadien-Styrol (SBS) und Ethylen-Vinylacetat (EVA). Die Untersuchungen haben gezeigt, dass bei einem Temperaturabfall die Werte der Bruchzähigkeit ansteigen und die Werte der maximalen vertikalen Verformungen sinken. Es wurde festgestellt, dass für beide eingesetzte Verfahren die tiefste Bruchzähigkeit bei der Verwendung des Bindemittels EVA auftritt.

Schlüsselwörter:
heiße Asphaltmischung, Verhalten bei tiefen Temperaturen, Modifikation, Bruchzähigkeit

1. Introduction

Many pavement distresses, described as rutting, moisture-induced damage, low temperature cracking etc., may appear on asphalt pavements that have been in use for an extended period of time. Thermal fatigue cracking is one of the major failure modes for asphalt pavements that are subjected to alternating heating and cooling, while low-temperature cracking is a serious distress mode in very cold regions [1-3]. Failure by low temperature cracking occurs as a result of thermal stress buildup in the pavement. Microcracks appear on the surface of the pavement in cases when this stress becomes equal to or greater than the tensile strength of pavement. Propagation of cracks through the pavement is likely to occur as a result of continuing low temperature cycles [4]. When water fills these cracks during winter, it freezes and ice lenses as well as frost heave may develop. This condition results in the loss of fines and formation of voids under the pavement, leading to reduction in load bearing capacity of the pavement. It is important to take appropriate measures during design of pavements to be used in cold regions. Otherwise cracking may cause very serious problems, such as poor ride quality, reduced service life, and high maintenance costs [5].

Polymeric materials can be used as modifiers in bitumen and hot mix asphalt (HMA) mixtures so that a wider performance range can be achieved [6-8]. When plastomers are incorporated into bitumen, the resultant structure is a rigid three dimensional network that resists deformation. However, structures with elastomeric features, i.e., those resisting permanent deformation and recovering the original shape after loading, are obtained by using elastomeric modifiers in bitumen [9]. Styrene-butadiene-styrene (SBS) and ethylene-vinyl-acetate (EVA) are two materials that are most frequently used for bitumen-modification purposes [10]. EVA has been revealed to be a good modifier that improves resistance to permanent deformation and thermal cracking of HMAs [11, 12]. EVA is a copolymer consisting of 5 to 50 wt. % of vinyl acetate (VA). Acetate groups in the ethylene chain decrease the crystallinity of the copolymer whose properties are controlled by the amount of VA present in the structure. As the VA content increases, the increase in flexibility accompanies the decrease in crystallinity of the copolymer. A flexible copolymer exhibits low melting points and heat seal temperatures, as well as reduced stiffness, tensile strength and hardness [13]. SBS, a copolymer of styrene and butadiene, has a rubbery structure with a three dimensional network of physical cross-links. In the copolymer, while polystyrene (PS) blocks impart strength to the resin, soft polybutadiene (PB) blocks provide elasticity [14].

The structure of PB block in the SBS copolymer can be adjusted by means of special catalysts. This involves partial transfer of the double bonds on the PB blocks to the side chains. It was found that this modification has many advantages for the PMBs, such as low viscosity and better compatibility at equivalent molecular weight, resistance to oxidation, and thermal stability [15, 16].

According to the loading conditions, i.e., speed and temperature, fracture mechanics is used to study the fracture mechanism of hot mix asphalts. Principles of linear-elastic fracture mechanics (LEFM) are applicable to HMAs for the temperatures of 1 °C or less, while elastic-plastic fracture mechanics (EPFM) principles are applied at convenient loading speeds for the temperatures of 25°C and above [17]. Fracture toughness is the ability of a material with a crack to resist fracture. When a stress intensity factor (K_1) exceeds fracture toughness (K_{IC}), fracture occurs according to LEFM principles. It is obvious that in order to meet requirements for a satisfactory service life, asphalt pavements should have high fracture toughness values so that they can withstand loads when exposed to an extended range of temperatures. Formation of localized asphalt damage can be observed when the temperature drops under a certain level. This condition, along with the change in the micro-structural stress mechanism, determines the fracture resistance behaviour of asphalt concrete with respect to temperature [18]. However, experimental studies revealed that LEFM is not valid for quasi-brittle materials such as concrete, rock and asphalt concrete because K_{Ic} depends on the size and geometry. The inapplicability of LEFM is due to existence of an inelastic zone, the fracture process zone (FPZ), in front of a crack in quasi-brittle materials. Several non-linear fracture mechanics models have been developed to characterize the FPZ. These models can be classified as the cohesive crack models and the effective crack models. Cohesive crack models simulate the FPZ by a closing pressure, which diminishes near the crack tip, while effective crack models simulate the FPZ by an effective crack length. The main aim of any approach is to determine the critical crack extension (size of FPZ) at peak load.

A long term cyclic fracture, due to cycling loading or change in temperature, and short term cyclic fracture, due to an abrupt drop of temperature along with contraction stresses, are two typical fracture models. Present study mainly deals with the short term cyclic fracture which is a one time fracture failure problem. The crack propagation resistance of pure and polymer modified mixtures is examined in this study by means of two different experimental techniques, and in accordance with the both LEFM and non-linear elastic fracture mechanics, as considered in the above discussion.

2. Experimental studies

2.1. Materials and sample preparation

The materials used in the experimental study were PG 58–34 bituminous binder, supplied by TUPRAS Batman Refinery; two SBS modifiers, i.e., Kraton D 1101 and Kraton MD 243, produced by Shell Chemical Co.; and Evatane®2805, a type of EVA modifier, produced by Arkema. For the production of modified bitumens, pure bitumen was mixed with a selected modifier for 60 minutes at 180 °C. The speed of the mixer was fixed to 1000 rpm throughout the mixing operation.

Malatya, a city in the eastern part of Turkey, was selected in the scope of this study as the area for application of the final binder. After taking traffic and climate conditions of the city into account, PG 70-22 was selected as the desired binder performance grade. The binder and hot mix asphalt design were made in this study according to Superpave method. It was reported in previous studies that 3-7 % SBS or 2-6 % EVA could be added to pure bitumen so that the permanent polymer phase can be obtained [19]. In order to compare the effects of additives on the HMA properties, and based on the information given in literature, the amount of additive was kept constant at 4 wt. % in all mixtures.

Table 1 shows results of the dynamic shear rheometer (DSR) and bending beam rheometer (BBR) tests for pure bitumen as well as mixtures modified with 4 % SBS D1101 (MB_{SBS-D}), SBS MD243 (MB_{SBS-M}) and Evatane®2805 (MB_{EVA}). As can be seen in the table, performance grades of MB_{SBS-D} and MB_{SBS-M} are the same, i.e., PG 70-34. However, the low temperature performance grade of mixture with MB_{EVA} was one level lower, namely PG 70-28. Thus, it can be stated that the performances of MB_{SBS-D} and MB_{SBS-M} are better than MB_{EVA} at low temperatures. It should be noted that all modified bitumens comply with the desired binder performance grade, PG 70-22.

Table 1. DSR and BBR test results.

DSR test results				
Temperature [°C]	**G*/sinδ [Pa] (specification limit min. 1000 Pa)**			
	PG 58-34	**MB_{SBS-D}**	**MB_{SBS-M}**	**MB_{EVA}**
58	1258	4890	4204	4534
70	-	1326	1183	1512
	G*/sin δ (Pa) RTFOT residue (specification limit min. 2200 Pa)			
58	7862	-	-	-
70	-	5599	5171	6862
	G*. sin δ (Pa*10^6) PAV PAV residue (specification limit max. 5 · 10^6 Pa)			
16	1.83	-	-	-
22	-	1.69	1.52	-
25	-	-	-	1.34
BBR test results				
Temperature [°C]	**m value (specification limit min. 0.300)**			
	PG 58-34	**MB_{SBS-D}**	**MB_{SBS-M}**	**MB_{EVA}**
-18	-	-	-	0.306
-24	0.309	0.314	0.325	0.277
-30	0.266	0.221	0.291	-
	Creep stiffness [MPa] (specification limit max. 300 MPa)			
-18	-	-	-	131.3
-24	108.3	144.7	98.5	160.6
-30	140.9	242.6	121.9	-
	Performance grades (PG)			
	58-34	70-34	70-34	70-28

Table 2. Rotational viscosity test results

Properties	Standard	PG 58-34	MB_{SBS-D}	MB_{SBS-M}	MB_{EVA}
Viscosity (cP, 135 °C)	ASTM D4402	275.0	1125.0	825.0	1250.0
Viscosity (cP, 165 °C)	ASTM D4402	112.5	350.0	262.5	375.0
Modification index ($\eta_{modified}$ / η_{pure}, on 135 °C)	-	-	4.09	3.00	4.55
Modification indexs ($\eta_{modified}$ / η_{pure}, on 165 °C)	-	-	3.11	2.33	3.33
Mixing temperature range [°C]	-	151-158	171-173	169–171	171-173
Compaction temperature range [°C]	-	129-140	167-169	163–166	167-169
Napomena: 1 centipoise [cP] = 0,001 pascal sekunda [Pa·s]					

In order to determine the mixing and compaction temperatures of hot mix asphalts, rotational viscometer tests were also conducted for the unaged pure and modified binders at 135 °C and 165 °C, respectively. Using the collected viscosity data, a temperature-viscosity graph with the corresponding trend line was drawn to interpret the temperature dependency of the viscosity. The plot was used to determine the mixing and compaction temperatures of the mixtures. According to literature, bitumen binders should possess viscosities of about 170 ± 20 cP for mixing and 280 ± 30 cP for compaction [20], (Note: 1 centipoise [cP] = 0.001 pascal second [Pa·s]). Based on this information and the temperature-viscosity graph, the mixing and compaction temperatures were identified for the corresponding viscosity values. Meanwhile, as can be seen in Table 2, the binder fulfilled the workability requirement stating that the viscosity value at 135 °C should not exceed 3 Pa·s (3000 cP), and so that workability could be maintained [21]. It should be noted that the viscosity of the binder increased with the use of the binders, in which case the mixing and compaction temperatures also increased. Physical properties of the crushed limestone aggregate used in the mixture are summarized in Table 3; the gradation is presented in Figure 1.

Table 3. Physical properties of aggregate

Properties	Standard	Specification limits	Coarse	Fine	Filler
Abrasion loss [%] (Los Angeles)	ASTM D 131	Max 30	27.8	-	-
Abrasion loss [%] (Micro deval)	ASTM D 6928	Max 15	13.6	-	-
Frost action [%] (with Na_2SO_4)	ASTM C 88	Max 10	5.8	-	-
Flat and elongated particles [%]	ASTM D 4791	Max 10	3		
Specific gravity [g/cm³]	ASTM C127		2.544	-	-
Specific gravity [g/cm³]	ASTM C128		-	2.571	-
Specific gravity [g/cm³]	ASTM D854		-	-	2.675

Table 4. Volumetric properties of pure and polymer modified mixtures

Mixture properties	Specification limits	Binder type			
		Neat	MB_{SBS-D}	MB_{SBS-M}	MB_{EVA}
Optimum binder content [%]		4.88	5.27	5.35	5.07
Volume of air voids, Va. [%]	4.0	4.04	4.09	4.09	3.99
Voids in mineral aggregate, VMA [%]	min. 14.0	14.61	15.39	15.50	14.86
Voids filled with asphalt, VFA [%]	65-75	72.37	73.42	73.63	73.13
Dust proportion (DP)	0.8-1.6	1.07	0.98	0.97	1.02
%Gmm@Nini. = 8 [%]	max. 89	85.71	85.62	85.52	85.09
%Gmm@Ndes. = 100 [%]	96	95.96	95.91	95.91	96.01
%Gmm@Ndes. = 160 [%]	max. 98	97.78	96.76	97.34	97.75

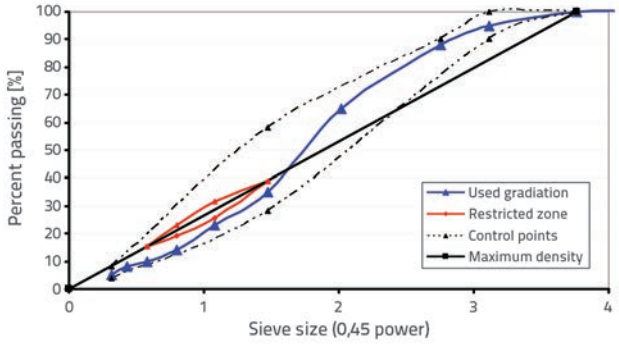

Figure 1. Combined aggregate gradation

In the scope of preparation of the HMAs, bitumen and aggregate were mixed at the mixing temperature (155 °C for neat mixture, 172 °C for mixtures prepared with MB_{SBS-D} and MB_{SBS-D}, and 170 °C for mixtures prepared with MB_{SBS-M}) using a special mixer. Uncompacted samples were placed on plates in an amount of 21-22 kg/m². Then, they were placed into an oven preheated to 135 °C, where they were short-term aged for 4 h. After ageing, the samples were compacted at the rate of 30 rpm by gyratory compactor having compaction angle of 1.25°. In the compaction process, vertical compression of 600 kPa was used for 100 rotations. Design binder contents (DBC) of compacted specimens were determined by means of their volumetric properties. As can be seen in Table 4, which shows volumetric properties and Superpave specification limits of the pure and polymer-modified mixtures, DBC values increase with the use of modified binder. The table demonstrates that all mixtures prepared within the scope of the study meet the Superpave specification criteria.

2.2. Semi-circular bending (SCB) test

The experimental procedure described in EN 12697–44 was used to measure the resistance of HMA specimens to crack propagation based on the concept of LEFM principles [22]. A gyratory compactor was used for preparation of specimens measuring 150 mm in diameter and 120 mm in thickness. Thus, the specimens contained 4 vol. % of air voids at the end of compaction. The compacted specimens were sliced into two equal semi-circular pieces. Then, the resulting semi-circular specimens were cut into two equal slices, each 50 mm in thickness. A single notch about 10 mm in depth and 1.5 mm in width was carved in the middle of the specimens. At the three-point loading configuration, the deformation was performed at the rate of 5.0 mm/min, see Figure 2 for the loading configuration details.

Three different temperatures, i.e., 0°C, -10°C and -20°C, were selected for the SCB test. Specimens were kept at the test temperature for 6 h before the testing. The load utilized and the corresponding deformation values were recorded throughout the SCB experiments. The fracture toughness (K_{IC}, N/mm$^{3/2}$) and maximum vertical strain values (ε_{max}, %) were calculated using the experimentally determined parameters, i.e., maximum stress value at failure (σ_{max}, N/mm²), maximum force value (F_{max}, N), and deformation value at maximum force (ΔW, mm). For this purpose, the following equations were used:

$$\sigma_{max} = \frac{4.263 * F_{max}}{D * t} \quad (1)$$

$$K_{IC} = \sigma_{max} \cdot 5{,}956 \quad (2)$$

$$\varepsilon_{max} = \frac{\Delta W}{W} \cdot 100 \quad (3)$$

where, D, W and t are the diameter, thickness and height of specimens in mm, respectively. The variation of the fracture toughness (K_{IC}) value with the type of additive and temperature is given in Figure 3.

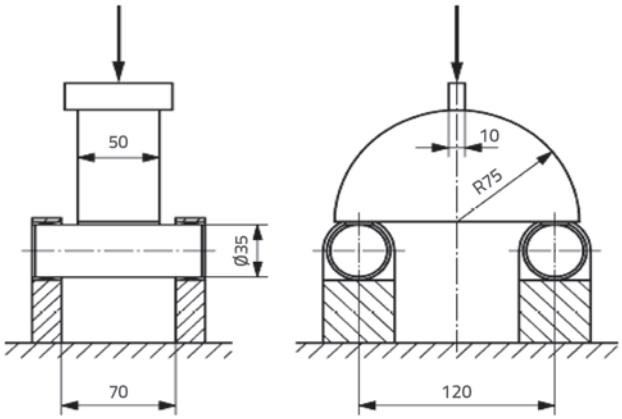

Figure 2. Semi-circular bending test configuration [22]

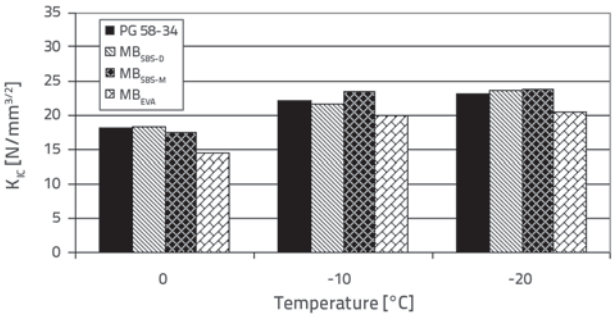

Figure 3. K_{IC} values of mixtures obtained by SCB test

As shown in Figure 3, the fracture toughness value increases with a decrease in temperature. At all temperatures, the lowest K_{IC} value was obtained in MB_{EVA} mixtures. The highest value, on the other hand, was obtained in MB_{SBS-D} at 0 °C and MB_{SBS-M} at -10 °C and -20 °C. At the temperature of 0 °C, the K_{IC} value of the control mixture (prepared with PG 58–34) was by 24.9 % higher than that of MB_{EVA}. Similarly, at the same temperature, the K_{IC} value of the mixture with MB_{SBS-D} was found to be by 26.5 % higher than that of the mixture with MB_{EVA} and by 20.9 % higher than that of mixture with MB_{SBS-M}. At the temperatures of -10 °C and -20 °C, the mixture with MB_{SBS-M}, which had the highest K_{IC} value overall, had the K_{IC} value by 17.9 % and 15.7 % higher than that of the mixture with MB_{EVA}, respectively.

It was detected that K_{IC} values increase significantly if the temperature drops from 0 °C to -10 °C. In such a case, the increase in the K_{IC} value was 22.9 %, 18.4 %, 34.1 % and 37.5 % for the mixture with pure bitumen (PG 58–34), MB_{SBS-D}, MB_{SBS-M} and MB_{EVA}, respectively. However, the increase was less significant when the temperature was changed from -10 °C to -20 °C. This was acquired if the increase in K_{IC} value was calculated for temperature drop from 0 °C to -20 °C. For this condition, it was detected that the increase was 27.8 %, 28.7 %, 35.9 % and 41.9 % for mixture with PG 58–34, MB_{SBS-D}, MB_{SBS-M} and MB_{EVA}, respectively. This also shows that the mixture with MB_{EVA} was affected the most by temperature drop. Variations of maximum strain (ε_{max}) values with temperature and the type of additive are given in Figure 4.

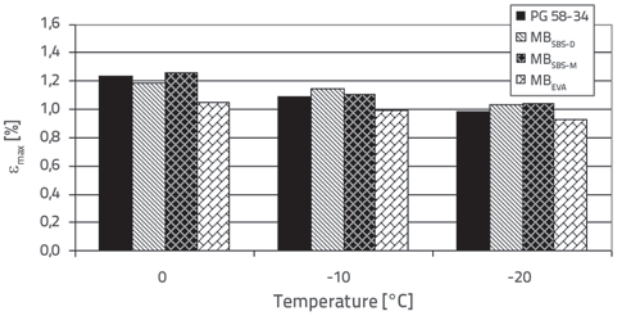

Figure 4. Maximum vertical strain (ε_{max}) values of mixtures

As shown in Figure 4, the mixture with MB_{EVA} had the smallest ε_{max} value at all temperatures. In contrast to that the highest value was obtained for MB_{SBS-M} at 0 °C as well as at -20 °C and for MB_{SBS-D} at -10 °C. At the temperatures of 0 °C and -20 °C, the ε_{max} value of the mixture with MB_{SBS-M} was by 19.8 % and 12.6 % higher than that of mixture with MB_{EVA}, respectively. It was found that the difference was 14.7 % at -10 °C.

It was observed that maximum strain values decrease with the decrease in temperature. When the temperature decreased from 0 °C to -10 °C, the decrease in ε_{max} value was 13.9 %, 3.5 %, 14.5 % and 5.6 % for the mixture with pure binder, MB_{SBS-D}, MB_{SBS-M} and MB_{EVA}, respectively. In case of temperature reduction from 0 °C to -20 °C, the decrease in K_{IC} value was 25.3 %, 14.5 %, 20.6 % and 13.4 % for the mixture with pure binder, MB_{SBS-D}, MB_{SBS-M} and MB_{EVA}, respectively. It can be seen that the ε_{max} value of the MB_{EVA} mixtures was affected the least from temperature drop, as the ε_{max} value of this mixture was rather small at all temperatures.

According to semi-circular bending tests, it can be stated that the mixtures with maximum resistance to crack propagation at 0 °C would be MB_{SBS-D}, while at -10 °C and -20 °C, such mixtures would be MB_{SBS-M}. In contrast to those, the resistance to crack propagation at low temperatures is fairly low for MB_{EVA} mixtures. Meanwhile, the experiments pointed out that with the addition of the elastomeric type of additives (Kraton D 1101 and Kraton MD 243), the ε_{max} value of the binder can be increased at lower temperatures, while the ε_{max} value decreases with the use of plastomeric type of additives (Evatane® 2805).

2.3. Single edge notched beam test

The single-edge notched beam (SE(B)) test geometry has been frequently applied [23, 24] for determining the fracture toughness value of asphalt concrete. Compared to other proposed geometries, this geometry yields more reliable results in the determination of fracture toughness, by providing simple loading configurations, by minimizing the edge effect by large dimensions and stable crack propagation in Mode I [25]. In fact, a standard was not previously set for determining fracture properties of prism shaped asphalt concrete. For this reason, dimensions used by Kim and Hussein (1997) were selected in this study as specimen dimensions [18]. To this end, first slab-shaped specimens measuring 30.5 × 30.5 × 5.0 cm were compacted by roller compactor to 4 vol. % of air voids. The amount of HMA necessary for slab specimens was calculated using the following equation:

$$M = 10^{-6} \cdot L \cdot l \cdot e \cdot \rho_m \cdot ((100 - v)/100) \quad (4)$$

where:

M - the weight of the specimen [kg]
L - the inner length of the mould [mm]
l - the inner width of the mould [mm]
e - the final height of the specimen [mm]
ρ_m - the maximum density of the bituminous mixture [kg/m^3]
v - the air voids of the specimen [%].

After the complete cooling of the specimen, it was cut to the required dimensions as given above. First, an insert positioned at the bottom centre of the beam mould was used to form a notch on the specimens having initial notch-depth (a_0) of 21 mm and initial notch-depth to beam-depth (W) ratio of 0.3. By using the three-point bending configuration, the specimens were deformed at a constant cross-head deformation rate of 3.24 mm/min. The configuration is shown in Figure 5. The loading span/notch depth ratio (S/W) of 4 was adopted in all deformation experiments.

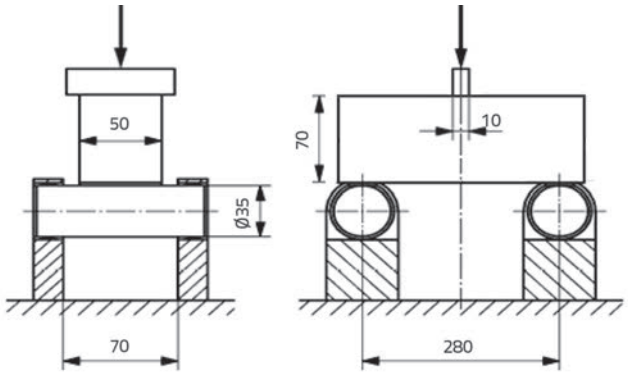

Figure 5. Single edge bending test configuration [18]

The effective crack model (ECM) was applied to determine the fracture behaviour of the specimens. By using P_i as $P_{max}/2$ [N], δ_i as deformation at P_i [mm]; B, W and S as width, depth and length of specimens [mm]; w as weight per unit length of beam, the Young's modulus (E) of the mixtures was calculated using the following equation [26]:

$$E = \frac{Pi}{4B\delta_i}\left(\frac{S}{W}\right)^3\left[1+\frac{5wS}{8P_i}+\left(\frac{W}{S}\right)^2\left[2{,}70+1{,}35\frac{wS}{Pi}\right]-0{,}84\left(\frac{W}{S}\right)^3\right] + \frac{9P_i}{2B\delta_i}\left(1+\frac{wS}{2P_i}\right)\left(\frac{S}{W}\right)^2 F_2(\alpha_0) \quad (5)$$

Here, the value of $F_2(\alpha_0)$ is determined as follows:

$$F_2(\alpha_0) = \int_0^{\alpha_0} \beta F_1^2(\beta)\, d\beta_1 \quad (6)$$

By using the known values of $\alpha_0 = a_0 / W$ and S/W, $F_1(\beta)$ can be re-written as

$$F_1(\beta) = \frac{1{,}99 - \beta(1-\beta)(2{,}15 - 3{,}93\beta + 2{,}70\beta^2)}{(1+2\beta)(1-\beta)^{1.5}} \quad (7)$$

process zone ahead of a visible crack are two main reasons for the reduction of beam stiffness. However, as it is rather difficult to distinguish between them, it is assumed that the critical notch depth (a_e) could be calculated by introducing a fictitious beam containing a notch a_e. It should be noted that, here, the notch has an unchanged stiffness that would be equal to the reduced stiffness of the real beam containing a notch of depth a_0, i.e.

$$\delta_{max} = \frac{P_{max}}{4BE}\left(\frac{S}{W}\right)^3\left[1+\frac{5wS}{8P_{max}}+\left(\frac{W}{S}\right)^2\left[2{,}70+1{,}35\frac{wS}{P_{max}}\right]-0{,}84\left(\frac{W}{S}\right)^3\right] + \frac{9P_{max}}{2BE}\left(1+\frac{wS}{2P_{max}}\right)\left(\frac{S}{W}\right)^2 F_2(\alpha_e) \quad (8)$$

where

$$F_2(\alpha_e) = \int_0^{\alpha_e} \beta F_1^2(\beta)\, d\beta_1 \quad (9)$$

It should be noted that the values of α_e *is* a_e */W* and $F_1(\beta)$ is directly obtained by using Equation 7. Then, the following equation can be applied to calculate the critical stress intensity factor (K_{IC}) of the specimens;

$$K_{IC} = \sigma_n \sqrt{a_e} F(\alpha) \quad (10)$$

where

$$\sigma_n = \frac{3(P_{max} + wS/2)S}{2bd^2} \quad (11)$$

Variations of maximum load values (P_{max}) of the mixtures with the type of additive and temperature are given in Figure 6. As shown in Figure 6, the maximum load value increases with the decrease in temperature. At all temperatures, the lowest value of P_{max} was obtained in MB_{EVA}. The highest value, on the other hand, was obtained in the mixture with MB_{SBS-D} at temperatures

of 0 °C and -10 °C. At -20 °C, the highest value was obtained in the mixture with MB_{SBS-M}. It was found that the P_{max} value of the mixture with MB_{SBS-D} was by 18.9 % and 15.4 % higher than those with MB_{EVA} at 0 °C and -10 °C, respectively. At -20 °C, the highest P_{max} value, obtained from the mixture with MB_{SBS-M}, was by 25 % higher than the lowest P_{max} value, which was obtained from the mixture with MB_{EVA}.

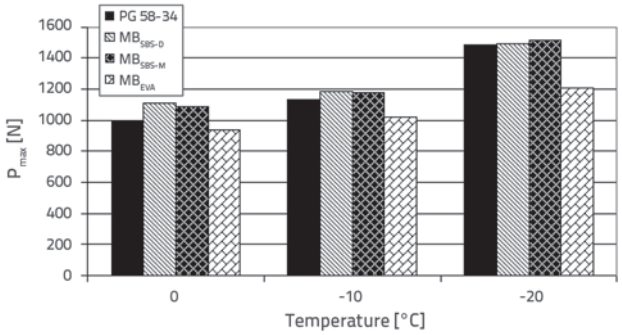

Figure 6. Variation of P_{max} values with type of additive and temperature

There was a significant increase in the P_{max} value when the temperature was decreased from -10 °C to -20 °C. In this condition, P_{max} values of the mixture with pure binder, MB_{SBS-D}, MB_{SBS-M} and MB_{EVA} increased by 31.2 %, 26.0 %, 28.3 % and 17.9 %, respectively. Similarly, when the temperature was decreased from 0 °C to -10 °C, P_{max} values of the mixture with pure binder, MB_{SBS-D}, MB_{SBS-M} and MB_{EVA}, increased by 12.6 %, 6.5 %, 8.9 % and 9.7 %, respectively. These results show that the mixture with pure binder was affected the most by temperature change in terms of P_{max} value. The variation of deformation (δ_{max}) value at maximum load with temperature is given in Figure 7.

As shown in Figure 7, the highest δ_{max} value was obtained in the mixture with MB_{SBS-D} at the temperature of 0 °C. At the temperatures of -10 °C and -20 °C, the highest value was registered for MB_{SBS-D} and MB_{SBS-M}, respectively. It was identified that at -10 °C, δ_{max} values of MB_{SBS-D} and MB_{SBS-M} were by 4.0 % and 3.3 % higher than that of the mixture, respectively. δ_{max} values decreased regularly with the decrease in temperature. The variation of fracture toughness values with the type of additive and temperature is given in Figure 8.

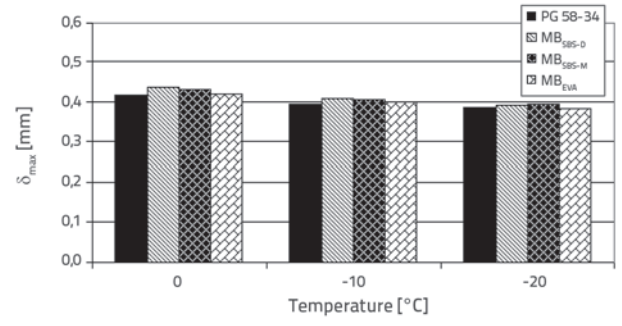

Figure 7. Vertical deformation at maximum load (δ_{max}) values of mixtures

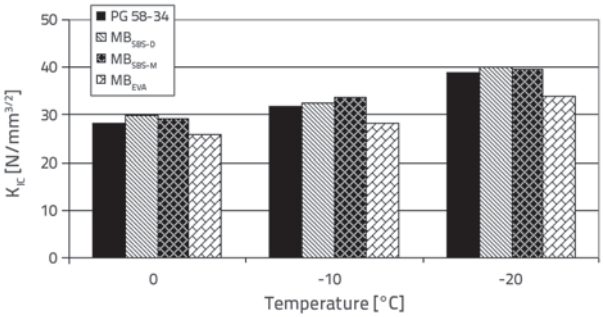

Figure 8. K_{IC} values of mixtures obtained at single edge bending test

Figure 8 shows that the K_{IC} value increases at all temperatures with the use of SBS in mixtures, while it decreases with the use of EVA. At the temperatures of 0 °C and -20 °C, the highest value was obtained in MB_{SBS-D}. It was found that at -10 °C, the highest value was obtained for the mixture with MB_{SBS-M}. At the temperatures of 0 °C and -20 °C, the K_{IC} value of the mixture with MB_{SBS-D} was by 15.8 % and 18.6 % higher compared to the one with MB_{EVA}, respectively. At -10 °C, the K_{IC} value of the mixture with MB_{SBS-M} was by 18.5 % higher compared to the one with MB_{EVA}, respectively.

K_{IC} values increased regularly with the decrease in temperature. When the temperature was decreased from 0 °C to -10 °C, K_{IC} values of the mixture with pure binder, MB_{SBS-D}, MB_{SBS-M} and MB_{EVA}, increased by 12.5 %, 9.1 %, 14.6 % and 10.0 %, respectively. Similarly, when the temperature was decreased from 0 °C to -20 °C, K_{IC} values increased by 38.0 %, 34.8 %, 35.4 % and 31.6 %, respectively.

2.4. Comparison of results of fracture mechanics tests

When compared with Figure 3 based on LEFM and Figure 8 based on the non-linear fracture mechanics, K_{Ic} values obtained from beam tests (approximately 30 $Nmm^{3/2}$) were greater than those of semi-circular bending tests (approximately 20 $Nmm^{3/2}$). This points to the existence of an inelastic zone (FPZ) in front of a crack in asphalt materials in even lower temperature ranges. The ECM based on non-linear fracture mechanics can also be employed to determine whether the quasi-brittle material behaviour is ductile or brittle. According to ECM, the relative length of FPZ (α_e - α_0) gives a good indication of brittleness. For instance, the length of FPZ is zero for perfectly brittle materials and LEFM is applicable.

As shown in Table 5, 6 and 7, the relative effective crack length (α_e) slightly decreases with the decrease in temperature. Consequently, it may be concluded that the beam specimens exhibit a more brittle behaviour with the decrease in temperature. However, it is well known that the tensile strength of asphalt materials, which is the most important parameter in cohesive crack approaches, increases with

the decrease in temperature. As clearly indicated in Table 5 and Table 6, the nominal strength values of beams highly increased with the decrease in temperature. Finally, it was concluded based on this discussion that the critical stress intensity factor values of the beam specimens increase with the decrease in temperature.

Table 5. SE(B) test results at 0°C

0°C									
Mixture type	**Sample No.**	P_i [N]	δ_i [%]	**E** [N/mm²]	P_{max} [N]	δ_{mak} [%]	σ_{Nc} [MPa]	α_e	K_{IC} [N/mm$^{3/2}$]
Neat	**1**	506.51	0.1027	3498	1013.01	0.4042	1.737	0.545	30.259
	2	476.48	0.1174	2909	952.97	0.397	1.630	0.516	25.76
	3	522.39	0.1277	2878	1044.78	0.4488	1.786	0.52	28.658
	Mean			**3095**	**1003.59**	**0.4167**			**28.226**
MB_{SBS-D}	**1**	575.44	0.1362	2927	1150.87	0.4335	1.973	0.495	29.103
	2	559.7	0.1345	2897	1119.41	0.4563	1.919	0.51	29.718
	3	531.83	0.1131	3297	1063.66	0.4231	1.820	0.533	30.389
	Mean			**3040**	**1111.31**	**0.4376**			**29.737**
MB_{SBS-M}	**1**	547.67	0.1181	3235	1095.34	0.4326	1.874	0.527	30.72
	2	523.86	0.1294	2838	1047.72	0.4217	1.787	0.504	27.162
	3	551.64	0.1291	2973	1103.29	0.4458	1.886	0.514	29.651
	Mean			**3015**	**1082.11**	**0.4333**			**29.178**
MB_{EVA}	**1**	425.58	0.1261	2475	851.17	0.414	1.456	0.514	22.915
	2	480.49	0.1227	2806	960.98	0.4261	1.647	0.521	26.481
	3	496.02	0.1172	3005	992.03	0.4169	1.696	0.525	27.621
	Mean			**2762**	**934.73**	**0.419**			**25.672**

Table 6. SE(B) test results at -10°C and -20°C

-10°C									
Mixture type	**Sample No.**	P_i [N]	δ_i [%]	**E** [N/mm²]	P_{max} [N]	δ_{mak} [%]	$\sigma_{Nχ}$ [MPa]	α_e	K_{IC} [N/mm$^{3/2}$]
Neat	**1**	575.05	0.1113	3566	1150.1	0.4066	1.962	0.525	31.957
	2	555.5	0.0927	4180	1111	0.3785	1.905	0.549	33.646
	3	564.1	0.1179	3329	1128.2	0.3947	1.934	0.507	29.66
	Mean			**3692**	**1129.77**	**0.3933**			**31.755**
MB_{SBS-D}	**1**	585.05	0.1087	3718	1170.1	0.4061	2.006	0.529	33.066
	2	602.4	0.1147	3594	1204.8	0.4196	2.055	0.524	33.305
	3	587.7	0.1183	3424	1175.4	0.4015	2.011	0.508	30.974
	Mean			**3579**	**1183.43**	**0.4091**			**32.448**
MB_{SBS-M}	**1**	578	0.1016	3938	1156	0.4001	1.982	0.54	33.944
	2	582.45	0.1032	3902	1164.9	0.4046	1.997	0.539	34.068
	3	606.8	0.1199	3475	1213.6	0.4146	2.080	0.511	32.338
	Mean			**3772**	**1178.17**	**0.4064**			**33.45**
MB_{EVA}	**1**	528.55	0.1134	3280	1057.1	0.3963	1.812	0.519	28.881
	2	550.45	0.1163	3291	1100.9	0.4012	1.878	0.514	29.539
	3	459.65	0.1108	2999	919.3	0.4016	1.576	0.532	26.269
	Mean			**3190**	**1025.77**	**0.3997**			**28.23**

Table 7. SCB test results at 0°C and -10°C

-20°C									
Mixture type	**Sample No:**	P_i [N]	δ_i [%]	**E** [N/mm²]	P_{max} [N]	δ_{mak} [%]	$\sigma_{N\chi}$ [MPa]	α_e	K_{IC} [N/mm$^{3/2}$]
Neat	**1**	764	0.1152	4406	1528	0.3855	2.619	0.497	38.843
	2	743.75	0.1059	4674	1487.5	0.3922	2.545	0.52	40.653
	3	715.55	0.1127	4243	1431.1	0.3892	2.446	0.506	37.366
	Mean			**4441**	**1482.2**	**0.389**			**38.954**
MB_{SBS-D}	**1**	737.25	0.1153	4266	1474.5	0.398	2.528	0.505	38.432
	2	727.8	0.1058	4597	1455.6	0.3961	2.495	0.523	40.225
	3	771.2	0.1048	4871	1542.4	0.3826	2.639	0.516	41.566
	Mean			**4578**	**1490.83**	**0.3922**			**40.075**
MB_{SBS-M}	**1**	733.35	0.1061	4606	1466.7	0.3863	2.509	0.517	39.642
	2	764	0.1179	4281	1528	0.3998	2.607	0.5	39.039
	3	770.6	0.1141	4465	1541.2	0.3932	2.635	0.503	39.868
	Mean			**4451**	**1511.97**	**0.3931**			**39.516**
MB_{EVA}	**1**	611.3	0.1161	3608	1222.6	0.3855	2.092	0.502	31.59
	2	639.55	0.1038	4199	1279.1	0.3872	2.193	0.526	35.754
	3	562.95	0.0946	4129	1125.9	0.3873	1.925	0.549	34.033
	Mean			**3978**	**1209.2**	**0.3867**			**33.792**

2.5. Comparison of experimental procedures of fracture mechanics

Fracture mechanics tests were performed in the scope of the study on both semi-circular and rectangular prism shaped samples using the principles of fracture mechanics. In both experiments, fracture toughness values were calculated at different temperatures. SE(B) test results are given in Table 5, 6 and 7. SCB test results are given in Table 8, 9 and 10. In order to elucidate the linear relationship and its strength between

Table 8. SCB test results at -20°C

0 °C					
Mixture type	**Sample No:**	F_{max} [N]	ε_{max} [%]	σ_{max} [N/mm²]	K_{IC} [N/mm$^{3/2}$]
Neat	1	5546.6	1.258	3.1506	18.765
	2	5252.3	1.226	2.9656	17.663
	3	5305.2	1.230	2.9837	17.771
	Mean	**5368.0**	**1.238**	**3.033**	**18.066**
MB_{SBS-D}	1	5243.4	1.253	2.9883	17.799
	2	5628.0	1.092	3.1694	18.877
	3	5401.4	1.210	3.0620	18.237
	Mean	**5424.3**	**1.185**	**3.073**	**18.304**
MB_{SBS-M}	1	5124.7	1.332	2.8689	17.087
	2	5211.9	1.150	2.9215	17.401
	3	5352.3	1.308	3.0181	17.976
	Mean	**5229.7**	**1.263**	**2.936**	**17.488**
MB_{EVA}	1	4606.5	1.039	2.5704	15.309
	2	4219.9	1.056	2.3655	14.089
	3	4166.3	1.069	2.3509	14.002
	Mean	**4330.9**	**1.055**	**2.429**	**14.467**

Table 9. SCB test results at -10°C

-10°C					
Mixture type	**Sample No:**	F_{max} [N]	ε_{max} [%]	σ_{max} [N/mm²]	K_{IC} [N/mm$^{3/2}$]
Neat	1	6696.3	1.067	3.7685	22.445
	2	6625.7	1.112	3.7411	22.282
	3	6497.2	1.082	3.6758	21.893
	Mean	**6606.4**	**1.087**	**3.728**	**22.207**
MB_{SBS-D}	1	6488.7	1.181	3.6808	21.923
	2	6437.7	1.119	3.6422	21.693
	3	6335.3	1.137	3.5914	21.390
	Mean	**6420.6**	**1.145**	**3.638**	**21.669**
MB_{SBS-M}	1	7040.1	1.061	3.9542	23.551
	2	6866.3	1.157	3.8591	22.985
	3	7100.5	1.091	3.9960	23.800
	Mean	**7002.3**	**1.103**	**3.936**	**23.445**
MB_{EVA}	1	5920.3	0.990	3.3406	19.897
	2	5752.6	0.978	3.2503	19.359
	3	6083.2	1.027	3.4280	20.417
	Mean	**5918.7**	**0.998**	**3.340**	**19.891**

Table 10. SCB test results at -20 °C

-20 °C					
Mixture type	**Sample No:**	F_{max} [N]	ε_{max} [%]	σ_{max} [N/mm²]	K_{IC} [N/mm$^{3/2}$]
Neat	**1**	6630.6	1.031	3.7414	22.284
	2	7157.4	0.979	4.0494	24.118
	3	6813.0	0.954	3.8418	22.882
	Mean	**6867.0**	**0.988**	**3.878**	**23.094**
MB_{SBS-D}	**1**	7145.0	1.011	4.0504	24.124
	2	7017.1	1.076	3.9516	23.536
	3	6890.5	1.019	3.8676	23.035
	Mean	**7017.6**	**1.035**	**3.957**	**23.565**
MB_{SBS-M}	**1**	7237.9	1.056	4.0706	24.245
	2	6869.3	0.995	3.8355	22.844
	3	7263.3	1.090	4.0635	24.202
	Mean	**7123.5**	**1.047**	**3.990**	**23.764**
MB_{EVA}	**1**	6144.0	0.910	3.4622	20.621
	2	6171.0	0.963	3.4614	20.616
	3	6090.0	0.918	3.4183	20.359
	Mean	**6135.0**	**0.930**	**3.447**	**20.532**

the values, determination coefficients and K_{IC} values equations for all mixtures were identified at the same temperature. Mean K_{IC} values were used in the assessment. The determination coefficients and equations are given in Figure 9.

The values displayed in Figure 9 were determined by Microsoft Excel linear regression analyses. Analysis results demonstrate that R^2 values are extremely high. The lowest value was identified at 0 °C (0.8641) and the value increased with the decrease in temperature. It was revealed by analysis results that K_{IC} values for SCB samples could be explained by K_{IC} values of SE(B) samples at the rate of 86.41 % and at 0 °C, whereas the same rate was 88.07 % and 98.06 % at -10 and -20 °C, respectively.

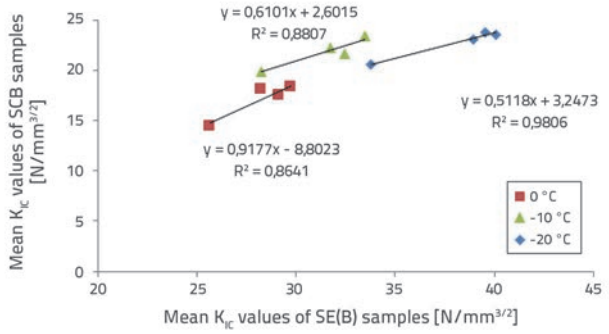

Figure 9. Linear regression parameters of K_{IC} values

Correlation coefficients (r) for K_{IC} values obtained from SCB and SE(B) samples at 0 °C, -10°C and -20°C were calculated. It was determined that these correlation coefficient values were 0.930, 0.938 and 0.990, respectively. These values demonstrated a positive correlation between K_{IC} values. Furthermore, the analysis of correlation strength demonstrated that r values were greater than 0.90 at all three temperatures (0 °C, -10°C and -20°C). Therefore, there was a strong correlation between the results obtained with both experimental methods. Furthermore, it was identified that the strength of this correlation increased with the decrease in temperature.

3. Conclusions

The low-temperature crack propagation resistance of control and polymer modified mixtures was examined in this study using two distinct experimental techniques. Within this scope, the design of binder and mixture was conducted using the Superpave method.

According to semi-circular bending tests performed, fracture toughness values increased with the decrease in temperature, while the maximum vertical strain values decreased. At all temperatures, the lowest K_{IC} value was obtained in MB_{EVA}. The highest value, on the other hand, was obtained in MB_{SBS-D} at 0 °C and MB_{SBS-M} at -10 °C and -20 °C.

Single edge notched beam experiments revealed that fracture toughness values based on ECM increase, while the maximum vertical deformation value decreases with the decrease in temperature. At all temperatures, the lowest K_{IC} value was obtained in MB_{EVA}. The highest value, on the other hand, was obtained in MB_{SBS-D} at 0 °C and -20 °C, MB_{SBS-M} at -10 °C.

When the effects of binders are compared, the experiments show that the low-temperature performance of MB_{SBS-D} and MB_{SBS-M} is higher compared to MB_{EVA}. The experiments in which mixtures were compared with each other showed that, at low temperature, the resistance to crack propagation increases with the addition of SBS type elastomers to pure mixtures. For EVA type plastomers, the resistance is lost to some extent. When the experimental procedures are compared, it can be stated that two techniques are coherent and approximately linear to one another.

Acknowledgements

This study was supported by Fırat University Scientific Research Projects Unit (FUBAP) under project number MF.12.01. The financial contribution of FUBAP is gratefully acknowledged.

REFERENCES

[1] Hribar, D., Tušar, M.: Properties of Asphalt Concrete at Low Temperatures, *Građevinar,* 64 (2012) 10, pp. 825-831.

[2] Hribar, D., Tušar, M., Hofko, B., Blab, R.: Influence of Start Temperature on Tensile Stress Testing of Restrained Asphalt Concrete Specimens, *Građevinar,* 65 (2013) 11, pp. 987-992.

[3] Ma, H., Wang, D., Zhou, C., Feng, D.: Calibration on MEPDG Low Temperature Cracking Model and Recommendation on Asphalt Pavement Structures in Seasonal Frozen Region of China, *Advances in Materials Science and Engineering,* Volume 2015, Article ID 830426, 11 pages, 2015.

[4] Das, P.K., Taşdemir, Y., Birgisson, B.: Low Temperature Cracking Performance of WMA with the Use of the Superpave Indirect Tensile Test, *Construction and Building Materials,* 30 (2012), pp. 643-649, https://doi.org/10.1016/j.conbuildmat.2011.12.013

[5] Isacsson, U., Zeng, H.: Relationships Between Bitumen Chemistry and Low Temperature Behaviour of Asphalt, *Construction and Building Materials,* 11 (1997) 2, pp. 83-91, https://doi.org/10.1016/S0950-0618(97)00008-1

[6] Polacco, G., Kriz, P., Filippi, S., Stastna, J., Biondi, D., Zanzotto, L.: Rheological Properties of Asphalt/SBS/Clay Blends, *Europan Polymer Journal,* 44 (2008) 11, pp. 3512–3521, https://doi.org/10.1016/j.eurpolymj.2008.08.032

[7] Sureshkumar, M.S., Filippi, S., Polacco, G., Kazatchkov, I., Stastna, J., Zanzotto, L.: Internal Structure and Linear Viscoelastic Properties of EVA/Asphalt Nanocomposites, *Europan Polymer Journal,* 46 (2010), pp. 621–633, https://doi.org/10.1016/j.eurpolymj.2009.12.024

[8] Yilmaz, M., Yalcin, E.: The Effects of Using Different Bitumen Modifiers and Hydrated Lime together on the Properties of Hot Mix Asphalts, *Road Materials and Pavement Design,* 17 (2016) 2, https://doi.org/10.1080/14680629.2015.1091376

[9] Airey, G.: Rheological Evaluation of Ethylene Vinyl Acetate Polymer Modified Bitumens, *Construction and Building Materials,* 16 (2002) 8, pp. 473-487, https://doi.org/10.1016/S0950-0618(02)00103-4

[10] Sengoz, B., Isıkyakar, G.: Evaluation of the Properties and Microstructure of SBS and EVA Polymer Modified Bitumen, *Construction and Building Materials,* 22 (2008) 9, pp. 1897-1905, https://doi.org/10.1016/j.conbuildmat.2007.07.013

[11] Singh, M., Kumar, P., Anupam, A.K.: Affect of Type of Aggregate on Permanent Deformation of Bituminous Concrete Mixes, *Road Materials and Pavement Design,* https://doi.org/10.1080/14680629.2015.1091374

[12] Topal, A.: Evaluation of the Properties and Microstructure of Plastomeric Polymer Modified Bitumens, *Fuel Processing Technology*, 91 (2010), pp. 45-51, https://doi.org/10.1016/j.fuproc.2009.08.007

[13] Doğan, M.: Effect of Polymer Additives on the Physical Properties of Bitumen Based Composites, Ankara, *M.Sc. Thesis*, Graduate School of Natural and Applied Sciences, Middle East Technical University, 2006.

[14] Airey, G.: Rheological Properties of Styrene Butadiene Styrene Polymer Modified Road Bitumens, *Fuel,* 82 (2003) 14, pp. 1709-1719, https://doi.org/10.1016/S0016-2361(03)00146-7

[15] Scholten, E.J., Vonk, W., Korenstra, J.: Towards Green Pavements with Novel Class of SBS Polymers for Enhanced Effectiveness in Bitumen and Pavement Performance, *International Journal of Pavement Research and Technology*, 3 (2010) 4, pp. 216-222.

[16] Vonk, W., Scholten, E.J., Korenstra, J.: Novel Class of SBS Polymers for Enhanced Effectiveness in Bitumen Modification, *Australian Asphalt Paving Association Thirteenth International Flexible Pavements Conference*, Queensland, Australia**,** 2010.

[17] Molenaar, J.M.M.: Performance Related Characterization of the Mechanical Behaviour of Asphalt Mixtures, *Rijkswaterstaat Road and Hydraulic Engineering Institute,* Delfth, Netherlands, 2003.

[18] Kim, K.W., Hussein, M.E.: Variation of Fracture Toughness of Asphalt Concrete Under Low Temperatures, *Construction and Building Materials,* 11 (1997) 8, pp. 403-411, https://doi.org/10.1016/S0950-0618(97)00030-5

[19] Lu, X., Isacsson, U.: Rheological Characterization of Styrene–Butadiene–Styrene Copolymer Modified Bitumens, *Construction and Building Materials,* 11 (1997) 1, pp. 23-32, https://doi.org/10.1016/S0950-0618(96)00033-5

[20] Zaniewski, J.P., Pumphrey, M.E.: Evaluation of Performance Graded Asphalt Binder Equipment And Testing Protocol, *Asphalt Technology Program,* 2004.

[21] Mc Gennis, R.B., Shuler, S., Bahia, H.U.: Background of Superpave Asphalt Binder Test Methods, *Report No:* FHWA-SA-94-069, 1994.

[22] EN 12697-44: Bituminous Mixtures - Test Methods for Hot Mix Asphalt – Part 44, Crack Propagation by Semi-Circular Bending Test, *European Standard,* 2010.

[23] Wagoner, M.P., Buttlar, W.G., Paulino, G.H.: Development of a Single-Edge Notched Beam Test for Asphalt Concrete Mixtures, *Journal of Testing and Evaluation,* 33 (2005) 6, pp. 1-9.

[24] Marasteanu, M., Falchetto, A.C., Moon, K.H.: Investigation of Low Temperature Cracking in Asphalt Pavements, *National Pooled Fund Study – Phase II,* 2009.

[25] Wagoner, M.P., Buttlar, W.G., Paulino, G.H.: Disk-Shaped Compact Tension Test for Asphalt Concrete Fracture, *Experimental Mechanics,* 45 (2005) 3, pp. 270-277, https://doi.org/10.1177/0014485105053205

[26] Karihaloo, B.L., Nallathambi, P.: Notched Beam Test: Mode-I Fracture Toughness, In Fracture Mechanics Test Methods for Concrete, *Report of Technical Committee 89*-FMT, RILEM, 1991.